Theoretical Study of the Reaction of H Atoms with Vibrationally Highly Excited HF Molecules†

Erika Bene and György Lendvay*

Institute of Structural Chemistry, Hungarian Academy of Sciences, H-1525 Budapest, P.O. Box 17, Hungary

Received: August 17, 2005; In Final Form: December 23, 2005

Vibrationally highly excited molecules react extremely fast with atoms and probably with radicals. The phenomenon can be utilized for selectively enhancing the rate of reactions of specific bonds. On the basis of quasiclassical trajectory calculations, the paper analyzes mechanistic details of a prototype reaction, H + HF(v). At vibrational quantum numbers v above 2, the reaction exhibits capture-type behavior, that is, the reactive cross section diverges as the relative translational energy of the partners decreases, both for the abstraction and for the exchange channel. The mechanism of the reaction for both channels is different at low and at high translational energy. At low vibrational energy, the reaction is activated, which is switched to capture-type at high excitation. The reason is an attractive potential that acts on the attacking H atom when the HF molecule is stretched. In contrast to the 6-SEC potential surface of Mielke et al., the switch cannot be observed on the Stark−Werner potential surface, due to a small artificial barrier at high H−HF separation, preventing the reactants from obeying the attractive potential and also proving the importance of the latter. The exchange reaction can be observed even when the total energy available for the partners is below the exchange barrier, because at low translational energies the product F atom of a successful abstraction step can re-abstract that H atom from the intermediate product H_2 molecule that was originally the attacker.

Introduction

Directing chemical reactions is one of the most important goals of chemists. In addition to the traditional ways of modifying the conditions of the reaction or using proper additives, recently physical—mostly spectroscopic—techniques became available to modify the course of reactions. One way of doing this is the application of properly shaped and timed light pulses *during* a chemical reaction (coherent control) that can be used in unimolecular processes (mostly photodissociation); another is the preparation of the reactants in appropriate quantum states *before* the reaction, which can also be used for bimolecular reactions. The former has seen a number of theoretical studies recently,[1−4] and successful applications have also appeared.[5,6] Governing reactions by preparing the reactants in various vibrational states for unimolecular processes is generally known as vibrationally mediated photodissociation[7] and has been used in many experiments. The preparation of reactants for bimolecular reactions was first explored experimentally,[8−19] while theoretical studies and the explanation for the observed phenomena followed later. In particular, Sinha et al.[7−9] demonstrated in relative rate measurements that the reaction of H atoms with HOD can be made bond selective by exciting the OH local stretch mode by 4 vibrational quanta: they observed OD formation, but no OH was detected. In related experiments Bronikowski et al.[12−15] generated fast H atoms that reacted with HOD excited by 1 vibrational quantum in the OH or OD mode and showed that the excited bond reacts much faster than the unexcited. Both these observations were in line with the early theoretical predictions by Schatz and coworkers[20,21] who used quasiclassical trajectory (QCT) calculations and found that selective vibrational excitation leads to selective enhancement of the rate and also agree with the quantum scattering calculations of Clary.[22] In sophisticated experiments under thermal conditions, Smith and co-workers[18,19,23] determined the absolute rate of the reaction H + H_2O(v) for several quantum states. They found that vibrational excitation enormously enhances the rate of the abstraction reaction, so that when the water molecule is excited by 4 quanta in the local O−H stretch mode, the room temperature rate coefficient is extremely large, 1.5×10^{-10} cm^3 molecule^{-1} s^{-1} close to the gas kinetic collision rate. The rate coefficient for the nonreactive removal of the $v = 4$ state is about twice as large. The first QCT calculations addressing the reproduction of these data failed,[24] which later[25] turned out to be due to the inadequacy of the early potential surfaces (PESs). By the use of two new potential surfaces,[25−27] QCT calculations[23] provided rate coefficients that were in good agreement with the experiments. These calculations also indicated that the long-range part of the potential is a very important factor responsible for the very large reaction rate. Remarkably, for the reverse reaction, OH + H_2, large vibrational enhancement of the rate was observed as well. Zellner and Seifert[28] as well as Glass and Chaturvedi[29] found that the rate can be enhanced by 2 orders of magnitude by exciting the H_2 vibration by one quantum.

In our previous studies,[30,31] we reported that the very large rate coefficients are due to a characteristic change of the excitation function when the vibrational excitation of the stretch mode participating in the reaction is gradually increased. The reaction switches from activated at low vibrational excitation to nonactivated at high excitation. We mean by this that at small stretch mode quantum numbers there is a nonzero translational threshold energy for reaction, while at high stretch excitation the reactive cross section diverges with decreasing translational energy like in capture processes,[32,33] indicating some kind of

* To whom correspondence should be addressed. E-mail: lendvay@chemres.hu.

† Part of the special issue "Jürgen Troe Festschrift".

10.1021/jp054638e CCC: $33.50
Published on Web 02/08/2006

TABLE 1: Properties of Stationary Points on the 6-SEC and SW Potential Surfaces

	6-SEC	SW
ΔE_{react}/kcal mol^{-1}	31.7	31.33
E_{barr}(abstraction)/kcal mol^{-1}	32.7	31.77
$r_{abs}^{\ddagger}$(H−H)/Å	0.757	0.771
$r_{abs}^{\ddagger}$(H−F)/Å	1.640	1.546
$\varphi_{abs}^{\ddagger}$(H−H−F)/deg	104.	119.
E_{barr}(exchange)/kcal mol^{-1}	37.34	41.1
$r_{exch}^{\ddagger}$(H−F)/Å	1.161	1.124
$\varphi_{exch}^{\ddagger}$(H−F−H)/deg	86.	180.

attractive force acting between the reactants under these conditions. This characteristic switch of the nature of the excitation function was found not to be specific to the reaction of highly vibrationally excited water. Similar behavior was also observed for the reverse reaction, for the reaction of H atoms with HF,

$$\mathrm{H} + \mathrm{H'F}(v) \rightarrow \mathrm{F} + \mathrm{HH'}\ \text{abstraction}$$
$$\rightarrow \mathrm{H'} + \mathrm{HF}\ \text{exchange}$$

which is in many respects analogous to that of H with water and even for the reverse reaction of the latter. In agreement with the earlier proposal,[25,26] the attractive potential that acts on the H atom already at large distances when the H′−F bond is stretched was found to be responsible for the extreme speed-up of the reaction. The large enhancement of the rate seems to be beyond that predicted by Polanyi's rules.[34−36] To provide a background for the general understanding of the possibilities of controlling rates of reactions by vibrational excitation of reactants, in the present paper, we investigate the details of the mechanism of the reaction of H atoms with vibrationally excited HF using QCT calculations. The H + HF reaction is particularly suited for theoretical studies as for this reaction well-known potential surfaces are available, and as long as one uses appropriate dynamical methods, the properties calculated can be presumed to be reliable. The H + HF abstraction reaction is highly endothermic (the experimental reaction heat is 31.73 kcal mol^{-1}). In the dynamical calculations, we used two potential surfaces, both of which are derived using ab initio calculations that recover essentially all correlation energy. One of them is the 6-SEC surface of Truhlar et al.,[37] the other is the potential surface developed by Stark and Werner[38] (hereafter referred to as SW PES). Some parameters of the two surfaces are compared in Table 1. Both potential surfaces predict a bent geometry for the saddle point of the abstraction channel, but the barrier height does not change by more than about one-half of a kcal mol^{-1} in a wide bending angle range. One difference between the two surfaces is that, while on the SW surface, the saddle point geometry for the exchange channel is collinear and bent arrangements follow a higher energy path, on the 6-SEC surface, wider angles are allowed and the real exchange barrier is at a highly bent geometry. The abstraction barrier is significantly shifted toward the product valley, the H−H bond is only 0.016 Å (6-SEC) and 0.030 Å (SW) longer, while the H−F bond is as much as 0.723 Å (6-SEC) and 0.628 (SW) Å longer at the saddle point than the equilibrium H−H and H−F bond lengths in the separated diatomic molecules. This type of potential surface is a typical example for which, according to Polanyi's rules, vibrational energy is favored for promoting the reaction.

In the rest of this paper, after briefly summarizing the technical details, we present some global characteristics of the reaction, like angular distributions, product state distributions, and a comparison of the abstraction and exchange channels, followed by a deeper view that is based on the analysis of the temporal history of numerous reactive and nonreactive collisions.

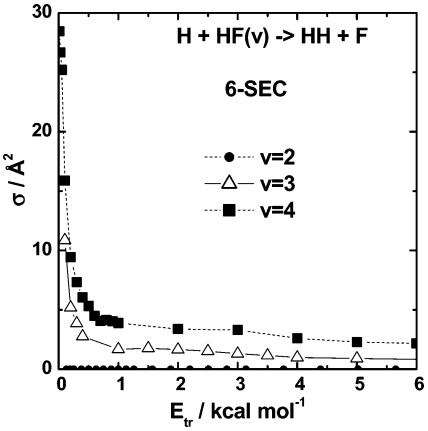

Figure 1. Excitation function for the H + HF(v) → F + H_2 reaction calculated on the 6-SEC potential surface for different vibrational states v of HF.

Methods

For the calculation of reactive cross sections, we used the standard QCT method. To rule out programming errors, we used two completely independent codes. One is an atom + diatom code originally written by J. M. Bowman and extensively enhanced by G. C. Schatz and one of the authors (G.L.); the other is an adaptation of the 1988 version of VENUS[39] that was parallelized[40] and streamlined for the present purpose. In all calculations, the connection between the orbital angular momentum and the initial impact parameter was considered to be purely classical. According to extensive tests, if the semiclassical connection between orbital angular momentum and impact parameter is used, then the results will not differ appreciably from those based on the purely classical connection (as long as there are enough trajectories to ensure reasonably small error limits). At every translational energy and vibrational quantum number, we determined the opacity function to make sure that the proper maximum impact parameter be used in the cross section calculations. In addition to the common quasiclassical setting of integer vibrational quantum numbers, we have set them to noninteger values to find out where the switch between the observed mechanisms takes place. The rotational quantum number of HF was set to the regular quasiclassical integer values. In this paper, we report the results obtained for nonrotating HF but the conclusions drawn are not specific to $j_{init} = 0$. It is worth noting that in addition to setting the time step appropriately, in calculations of this type, one needs to set the maximum allowed number of time steps to an unusually large value, otherwise at low translational energies the majority of reactive collisions are lost.

Standard ab initio calculations at the QCISD(T)/cc-pVQZ level were performed using the Gaussian98 suite of programs.[41]

Results

The excitation functions for the abstraction reaction obtained on the 6-SEC PES are shown in Figure 1 at three H′F vibrational quantum numbers. One can observe that at $v = 2$ the reactive cross section is very small (the threshold energy for reaction is about 5 kcal mol^{-1} and the cross sections remain below 0.5 Å^2 even at large translational energies). In contrast, at $v = 3$ or 4, the cross sections are, especially at low translational energy (at $E_{tr} = 0.005$ kcal mol^{-1} and $v = 4$), $\sigma = 73$ Å^2, an unusually

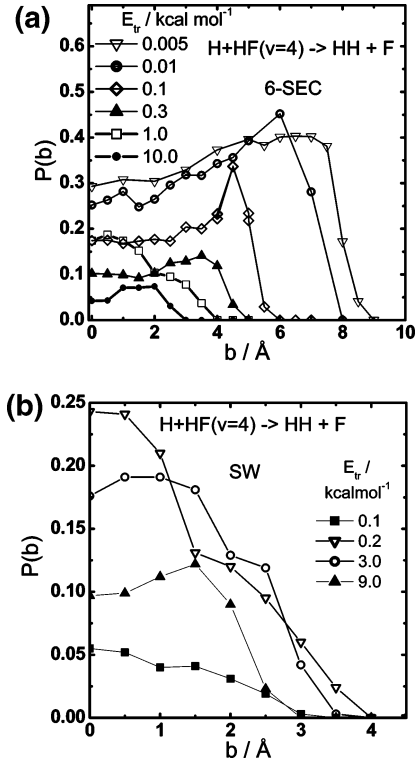

Figure 2. Opacity function for the $H + HF(v = 4) \rightarrow F + H_2$ reaction at various initial relative kinetic energies as obtained on the (a) 6-SEC and (b) SW potential surfaces.

large value for an abstraction reaction. The huge reactive cross sections are due to the very large impact parameter range that allows reaction, as the opacity functions at various translational energies show in Figure 2a. For comparison, in Figure 2b, we plotted the opacity functions obtained on the SW surface. While on the 6-SEC surface, the opacity function at low translational energies peaks at large impact parameters (as large as 7 Å); on the SW PES, the reactivity is concentrated in the low-impact parameter range. This is also reflected in the excitation functions obtained on the SW surface. As in ref 31, we calculated the reactive cross sections at various noninteger vibrational quantum numbers to determine when the switching occurs between the activated and capture-type behavior. Figures 3 and 4 show the comparison of the excitation functions for abstraction and exchange at vibrational quantum numbers between 2 and 3 obtained on the 6-SEC and SW PES, respectively. Several remarkable differences can be observed between the results on the two surfaces. First, while on the 6-SEC PES, the cross sections in the capture domain diverge with decreasing E_{tr}, on the SW PES, they fall off after a rise when E_{tr} is decreased, so that the switch to capture-type behavior does not take place. As shown later, we think this is a consequence of a low, but unphysical, barrier in the long-range part of the SW PES that shields the HF molecule from the attacking H atom. Another difference is that on the SW PES the exchange reaction is much less favored than on 6-SEC. This probably is caused by the larger cone of acceptance on 6-SEC, which results from a much smaller angle dependence of the height of the fixed-angle barrier. In other words, the fixed-angle barrier height remains within a small range (e.g., 0.5 kcal mol^{-1}) for a much larger bending angle range on 6-SEC than on SW. Concerning the location of the switch from activated to capture on the 6-SEC PES, one can see that as soon as the vibrational energy in the HF molecule exceeds the barrier (32.7 kcal mol^{-1}, see Table 1) at $v = 2.5$ ($E_{vib} = 33.3$ kcal mol^{-1}, see Table 2), the excitation function

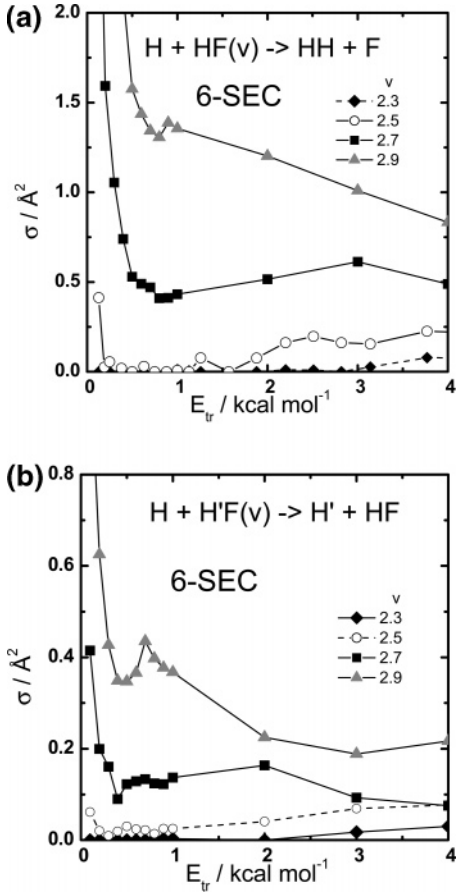

Figure 3. Excitation function for the $H + HF(v) \rightarrow F + H_2$ abstraction and $H + H'F(v) \rightarrow H' + HF$ exchange reactions at different noninteger vibrational quantum numbers v of the HF molecule around the switch from activated to capture-type behavior, obtained on the 6-SEC PES: (a) abstraction and (b) exchange.

becomes capture-type. This indicates that the vibrational energy can be converted into kinetic energy to overcome the barrier. Note, however, that the capture-type increase takes place only at very low translational energies at $v = 2.5$, which means that the enhancement of reactivity can manifest itself only when the partners spend an extended time together, that is, they have "enough time to notice each other". Interestingly, on the 6-SEC PES, the exchange process also shows capture-type behavior. Moreover, a nonvanishing exchange cross section can be observed at energies that are too low to exceed the barrier. For example, at $v = 2.7$ the cross section is not zero below $E_{tr} =$ 0.2 kcal mol^{-1}, even though the total energy in the system ($E_{tr} + E_{vib} = 35.3$ kcal mol^{-1}, see Table 2) is lower than the barrier for exchange (37.34 kcal mol^{-1}). At low translational energies, H-atom exchange can be observed even at as low a v value as 2.5 but not if the vibrational excitation is lower than that. In other words, the switch from activated to capture-type occurs at the same vibrational energy for abstraction and exchange, even though the barriers differ. We return to this question later.

The dynamics of both the abstraction and exchange reaction does not only change from activated to capture-type but also there is a difference between the mechanism at low and at large translational energies, as the opacity functions already indicate: at low E_{tr}, large impact parameter collisions dominate; at high E_{tr}, mostly collisions at a small impact parameter are reactive. The difference of the mechanisms can also be seen in the angular distributions (Figure 5), but the product vibrational distributions also change. At low translational energies, the angular distributions show forward−backward symmetry, but

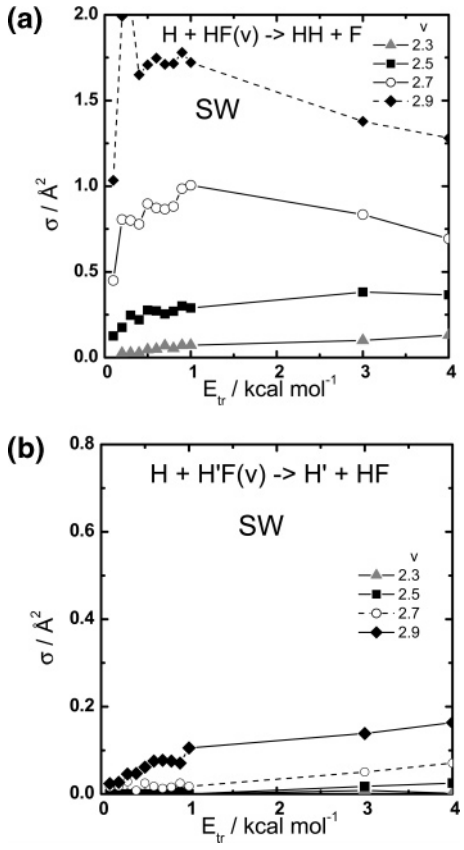

Figure 4. Same as Figure 3 but obtained on the SW PES: (a) abstraction and (b) exchange.

TABLE 2: Properties of Vibrationally Excited States of the HF Molecule

v	energy/ kcal mol^{-1}	H−F distance at outer turning point/Å
0	5.9	1.02
1	17.2	1.11
2	28.0	1.19
2.3	31.2	1.21
2.5	33.3	1.22
2.7	35.3	1.23
2.9	37.4	1.24
3	38.4	1.25
4	48.2	1.31

the investigation of individual trajectories indicates that this is not due to the formation of a long-lived complex in the usual sense (see later). At large translational energies, backward scattering dominates (just as when the vibrational energy of HF is low, see Figure 5b), reflecting that small impact parameter collisions determine the global dynamics. The vibrational distributions calculated at low and high translational energies are also characteristically different: at low E_{tr}, the product's vibrational distribution peaks around the same vibrational quantum number as that of the reactant HF, while at higher E_{tr}, reactive collisions exhibit a smaller degree of vibrational adiabaticity.

Discussion

The dissimilarity of the results obtained on the 6-SEC and the SW PES indicates that there is a specific difference on the otherwise very similar surfaces that changes the low-energy dynamics and prevents the total switch to capture-type behavior on the SW PES. We note that our quantum scattering calculations that are in progress using the two potential surfaces also

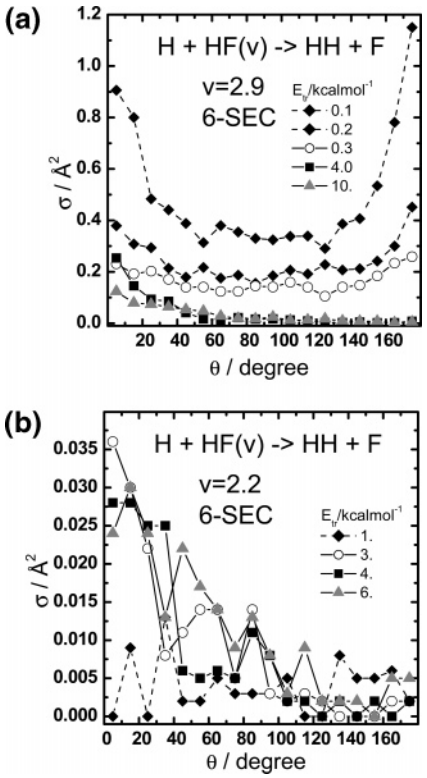

Figure 5. Angular distributions of the products of the H + H′F(v) abstraction at various translational energies at high (panel a) and low (panel b) vibrational quantum states of HF obtained on the 6-SEC potential surface.

indicate that the cross sections drop at very low translational energy on the SW PES, so that the phenomenon is probably not an artifact due to the use of classical mechanics. The reason for the change in dynamics is found in the potential observed by the H atom when it approaches a H′F molecule when the latter is stretched. Figure 6a shows a comparison of this region of the two surfaces, the energy of the collinear H−H′F system as a function of the H−H′ distance when the H′−F distance is fixed at various values up to 1.3 Å, close to the outer turning point of the H′F($v = 4$) vibration. On the SW PES, there is a small barrier (at most 0.3 kcal mol^{-1}) at large distances that is missing on the 6-SEC surface. Actually, there is an indication of this barrier in Figure 10 of ref 38. A detailed view of this region of the SW PES is shown in Figure 6b. We think that the barrier is not physical, instead, it is probably an artifact created by the fitting function used to smooth this region of the PES where there were too few ab initio points. To test this assumption, we performed QCISD(T)/cc-pVQZ calculations (presented in Figure 6c) and found no sign of any barrier. This level of calculation is high enough and certainly would indicate if there was a barrier in this region. As the earlier studies using the SW PES mostly addressed the reverse F + H_2 reaction, this feature did not cause serious problems and people probably have not even noticed it. It was only recently that in precise comparisons between high-quality exact quantum simulations and high-quality experiments on the F + H_2 reaction Skodje et al.[42] observed that the differences can be assigned to the small barrier in the product valley. They generated a modified version of the SW PES which we started using for dynamical calculations.

The very large influence of the small barrier at large distances corroborates the assumption proposed earlier[25,26,30,31] that the enormous enhancement of the rate is due to the long-range attractive part of the PES. Figure 7 shows the contour plot of

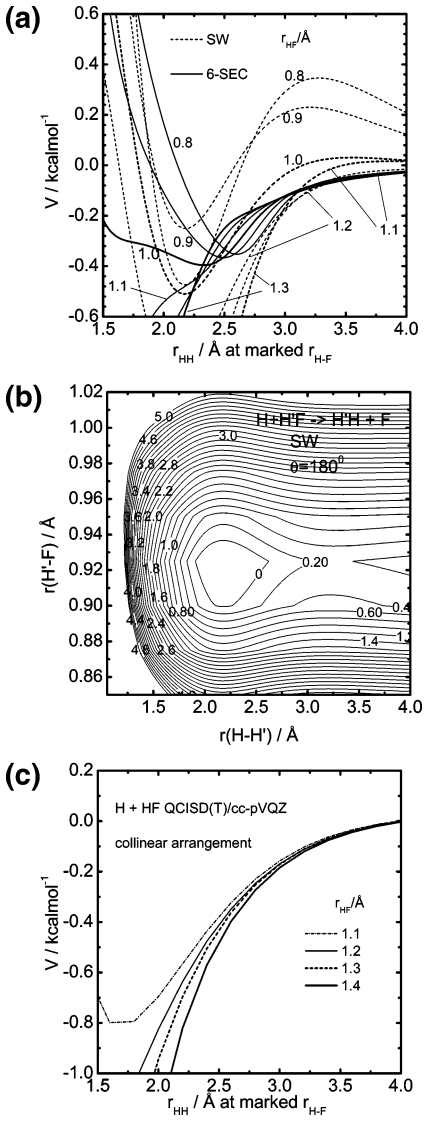

Figure 6. Sections of the H + HF → F + H_2 potential surface calculated for the collinear arrangement. The H−F distance is fixed and the H−H distance is varied: (a) 6-SEC PES (dashed lines) and SW PES (dashed lines); (b) a section of the SW PES at the collinear arrangement showing the unphysical barrier (energy in kcal mol^{-1}); (c) results of QCSID(T)/cc-pVQZ ab initio calculations. The energy is measured from the energy of the separated HF molecule at the selected H−F distance.

the 6-SEC PES at the H−H′−F angle of 104° (corresponding to the saddle point). It is worth noting that the surface at other angles does not show visible differences as compared to this one. To understand the influence of the shape of the potential surface on the dynamics, we marked in Figure 7 with a dashed line the location of the line corresponding to the approach of the attacking H atom toward the H′−F molecule stretched to 1.3 Å, which is the outer turning point of the H′F vibration at $v = 4$. The shape of the outer section of the potential curve along this line can be seen in Figure 6a on the attractive curve corresponding to r(H′−F) = 1.3 Å. The attraction is caused by the shape of the PES: at large H−F distances near the corner region of the PES, the outer contour lines continuously turn away from the horizontal axis, that is, when one approaches the corner region from large distances along the dashed line, the energy continuously decreases, in a sense guiding the incoming particle onto the barrier, and making the outer corner of the PES less sharp and easier to pass. This shape does not

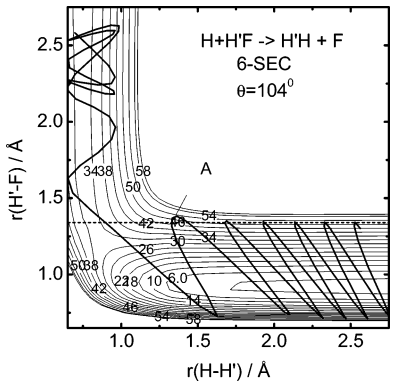

Figure 7. Cross section of the potential surface of the H + H′F(v) → HH′ + F reaction taken at the H−H′−F bond angle of 104° (the bending angle at the saddle point). Energy is shown in units of kcal mol^{-1}. The continuous black line represents a trajectory started at v(H′F) = 4. The dashed line corresponds to the H′F distance of 1.34 Å, which is the outer turning point of the H′F vibration at $v = 4$.

characterize all potential surfaces, and even in this PES, the contour lines at lower energies close to the barrier turn a little bit back toward the horizontal axis near the barrier, making the approach of the barrier less feasible for the incoming particle. It would be appealing to think that the less sharp corner of the higher-energy contour lines enables corner-cutting trajectories. We animated a number of trajectories confined to the collinear surface (which shows the same characteristics), but no corner-cutting was observed. Instead, collinear trajectories tend to oscillate exactly in the corner region many times before they end up in the product valley. It should be noted, however, that collinear trajectories are very rare and most reactions occur at a bent arrangement, yet corner-cutting is not the dominant mechanism for the enhanced reactivity. The influence of the attractive potential that the H atom experiences when the H′F bond is stretched, however, is clearly visible when one studies the large impact parameter collisions at very low translational energy. The incoming H atom changes its original direction of motion when still very far from H′F, and turns toward it, tracing a spectacularly curved path, clearly indicating the attraction. Figure 7 shows a typical trajectory calculated at $E_{tr} = 0.005$ kcal mol^{-1} with the H atom starting 10 Å away from H′F, arriving at a large impact parameter (7 Å). The figure shows the segment of the trajectory after the H has turned toward the H′F and approached it. It is worth noting that a large portion of the reactive trajectories started with similar impact parameters and translational energies trace essentially the same path, indicating that they follow the same scenario. The H atom is close to H′F for several vibrational periods. When the system is close to the outer repulsive corner on the potential surface (H close enough, H′F is stretched), the H atom can attract the H′ a little farther from the F atom than the regular outer vibrational turning point but cannot drag it. It is here (point A in Figure 7) when the steep inner section of the attractive potential curve shown in Figure 6 exerts its influence. The H′F performs one more vibration, but when the bond stretches, the H′ atom hits the H that is a little closer than it was at the previous encounter and they depart together. Most of the time the reaction occurs at a bent H−H′−F arrangement and the product HH′ rotates fast. The relative velocity of the products is larger than what the height of the barrier to the reverse reaction could explain. The extra energy comes from conversion of vibrational energy into translation, corresponding to reduced vibrational adiabaticity. Very few collisions form a long-lived collision complex defined as those characterized by multiple inner (and

outer) turning points of the H′−F and H−H′ oscillations. Interestingly, in the close encounter (i.e., what happens when the partners are close, like in the trajectory segment shown in Figure 7), the product HH′ molecule is almost always backscattered. The total angle of deflection (from the direction of approach to the direction of departure), however, is almost random, because the incoming H changes course very early and the close encounter occurs after an almost random period of time. This is the reason for the forward−backward symmetry on the low-energy angular distributions.

Another important phenomenon can be observed at relatively low vibrational and translational energies. As discussed above, Figure 3b shows that the trajectory calculations detect a nonzero cross section for the exchange reaction that seems not be allowed energetically at relatively low vibrational excitation of HF and low relative translational energy. More precisely, when E_{tr} is small, the sum of E_{tr} and E_{vib} is lower than the exchange barrier below $v = 2.8$, yet, a reaction is observed for vibrational energies corresponding to as low as $v = 2.5$. Such a phenomenon cannot be observed for the abstraction reaction. Vibrational adiabaticity cannot be the source of the missing energy as the entire vibrational energy plus the relative translation together is still not enough to surpass the barrier. Classical trajectories cannot account for tunneling, so there must be another mechanism for these processes. Visualization of many such trajectories revealed that the exchange reaction takes place in essentially two steps, neither of which is exchange itself. Instead, one can observe an H + H′F → HH′ + F abstraction and an F + HH′ → HF + H′ back-abstraction reaction. In more detail, when the H atom approaches the H′ of H′F, it generally arrives at an angle to the H′F bond. As a result, if the conditions are appropriate for abstraction of the H′, then the HH′ molecule that is formed will rotate. When the relative translational energy is small, the F atom departs slowly and it is often still close when the HH′ makes a half-turn and its H end points toward the F atom. If at this point the HH′ happens to be near the outer turning point of its vibration, then the F atom captures the H atom and the net reaction will be an H/H′ exchange in hydrogen fluoride. (Note that in numerous collisions the H′ atom is also re-abstracted, but the net result of such collisions is the "formation" of the reactants, H and H′F, that is, they are virtually nonreactive events and will not be observable experimentally.) As the translational energy increases, the chance that the HH′ is still close to the F when the products depart decreases and the "double abstraction" mechanism becomes less operative. On the other hand, the "real" exchange channel becomes open, so that the exchange reaction will take place in collisions when the H atom approaches on the F end of H′F. At large translational energy, the "double abstraction" mechanism does not play any role.

Conclusion

We made a detailed study using quasiclassical trajectories of the H + H′F reaction at large H′F vibrational energies with the purpose of connecting the extremely large vibrational enhancement of the rate with the features of the potential surface. The characteristic change in the excitations functions also observed for other reactions, namely, that the reaction is activated when the H′F vibrational energy is low and capture-type when E_{vib} is large, can be seen for this reaction on the 6-SEC potential surface but not on the SW surface, due to a small unphysical barrier at large distances on the latter. In addition to other observations, this also supports the assumption that the large vibrational enhancement of the rate is due to the long-range attraction that the incoming H atom experiences when approaching the vibrationally excited H′F molecule that is often stretched significantly. The consequence is that at low translational energies the reaction probability is large at very large impact parameters resulting in "inverted" opacity functions that peak at large impact parameters. The capture-type behavior observed at large vibrational excitation is completely analogous to collisions of two particles attracting each other. The enhanced reactivity of the vibrationally excited diatomic molecule and the long interaction time at low translational energies make possible the occurrence of an H atom exchange reaction at total energies below the barrier height of the direct exchange process taking place in two microsteps: the attacking H atom abstracts the H′ atom from F, turns, and the F atom abstracts the H of the HH′ formed in the previous microstep. We are performing additional calculations including quantum scattering to get a further insight into the dynamics of the reactions of reactants that are vibrationally excited, which is one way of directing chemical reactions into desired channels.

Acknowledgment. This work has been supported by the Hungarian National Research Fund (Grant No. OTKA T34812). We thank Dr. Ákos Bencsura for invaluable help with program development. G.L. thanks Prof. George C. Schatz and Dr. Diego Troya for helpful discussions made possible by the NSF-Hungarian Scientific Research Fund-Hungarian Academy of Sciences collaboration (Grant No. 006.)

References and Notes

(1) Rice, S. A.; Zhao, M. *Optical Control of Molecular Dynamics*; Wiley: New York, 2000.
(2) Brumer, P.; Shapiro, M.; Hepburn, J. W. *Chem. Phys. Lett.* **1988**, *149*, 451.
(3) Rabitz, H. *J. Mod. Opt.* **2004**, *51*, 16.
(4) Manz, J.; Paramanov, G. K. *J. Phys. Chem.* **1993**, *97*, 12625.
(5) Assion, A.; Baumert, T.; Bergt, M.; Brixner, T.; Kiefer, B.; Seyfried, V.; Strehle, M.; Gerber, G. *Science* **1998**, *282*, 919.
(6) Daniel, C.; Full, J.; González, L.; Lupulescu, C.; Manz, J.; Merli, A.; Vajda, S.; Wöste, L. *Science* **2003**, *299*, 536.
(7) Crim, F. F. *Annu. Phys. Chem.* **1993**, *44*, 397.
(8) Sinha, A. A.; Hsiao, M. C.; Crim, F. F. *J. Chem. Phys.* **1990**, *92*, 6334.
(9) Crim, F. F.; Hsiao, M. C.; Scott, J. L.; Sinha, A.; Vander Wal, R. L. *Philos. Trans. R. Soc. London, Ser. A* **1990**, *332*, 259.
(10) Sinha, A.; Hsiao, M. C.; Crim, F. F. *J. Chem. Phys.* **1991**, *94*, 4928.
(11) Hsiao, M. C.; Sinha, A.; Crim, F. F. *J. Phys. Chem.* **1991**, *95*, 8263.
(12) Bronikowski, M. J.; Simpson, W. R.; Zare, R. N. *J. Chem. Phys.* **1991**, *95*, 8647.
(13) Metz, R. B.; Thoemke, J. D.; Pfeiffer, J. M.; Crim, F. F. *J. Chem. Phys.* **1993**, *99*, 1744.
(14) Bronikowski, M. J.; Simpson, W. R.; Zare, R. N. *J. Phys. Chem.* **1993**, *97*, 2194.
(15) Bronikowski, M. J.; Simpson, W. R.; Zare, R. N. *J. Phys. Chem.* **1993**, *97*, 2204.
(16) Thoemke, J. D.; Pfeiffer, J. M.; Metz, R. B.; Crim, F. F. *J. Phys. Chem.* **1995**, *99*, 13748.
(17) Adelman, D. E.; Filseth, S. V.; Zare, R. N. *J. Chem. Phys.* **1993**, *98*, 4636.
(18) Hawthorne, G.; Sharkey, P.; Smith, I. W. M. *J. Chem. Phys.* **1998**, *108*, 4693.
(19) Barnes, P. W.; Sharkey, P.; Sims, I. R.; Smith, I. W. M. *Faraday Discuss.* **1999**, *113*, 167.
(20) Schatz, G. C.; Colton, M. C.; Grant, J. L. *J. Phys. Chem.* **1984**, *88*, 2971.
(21) Kudla, K.; Schatz, G. C. *J. Chem. Phys.* **1993**, *98*, 4644.
(22) Clary, D. C. *Chem. Phys. Lett.* **1992**, *192*, 34.
(23) Barnes, P. W.; Sims, I. R.; Smith, I. W. M.; Lendvay, G.; Schatz, G. C. *J. Chem. Phys.* **2001**, *115*, 4586.
(24) Lendvay, G.; Bradley, K. S.; Schatz, G. C. *J. Chem. Phys.* **1999**, *110*, 2963.
(25) Schatz, G. C.; Wu, G.; Lendvay, G.; Fang, D.-C.; Harding, L. B. *Faraday Discuss.* **1999**, *113*, 151.
(26) Wu, G.; Schatz, G. C.; Lendvay, G.; Fang, D. C.; Harding, L. B. *J. Chem. Phys.* **2000**, *113*, 3150; Erratum, *J. Chem. Phys.* **2000**, *113*, 7712.

(27) Ochoa de Aspuru, G.; Clary, D. C. *J. Phys. Chem. A* **1998**, *102*, 9631.
(28) Zellner, R.; Steinert, W. *Chem. Phys. Lett.* **1981**, *58*, 568.
(29) Glass, G. P.; Chaturvedi, B. K. *J. Chem. Phys*. **1981** *75*, 2749.
(30) Bene, E.; Lendvay, G.; Póta, G. In *Theory of Chemical Reaction Dynamics*; Laganà, A., Lendvay, G., Eds.; Kluwer: Dordrecht, The Netherlands, 2004; pp 349−361.
(31) Bene, E.; Lendvay, G.; Póta, G. *J. Phys. Chem. A* **2005**, *109*, 8366.
(32) Clary, D. C. *Chem. Phys. Lett.* **1995**, *232*, 267 and references therein.
(33) Troe, J. In *Theory of Chemical Reaction Dynamics*; Laganà, A., Lendvay, G., Eds.; Kluwer: Dordrecht, The Netherlands, 2004; pp 399−411.
(34) Polanyi, J. C. *Acc. Chem. Res.* **1972**, *5*, 161.
(35) Kuntz, P. J.; Nemeth, E. M.; Polanyi, J. C.; Rosner, S. D.; Young, C. E. *J. Chem. Phys.* **1966**, *44*, 1168.
(36) Smith, I. W. M. *Kinetics and Dynamics of Elementary Gas Reactions*; Butterworth: London, 1980.
(37) Mielke, S. L.; Lynch, G. C.; Truhlar, D. G.; Schwenke, D. W. *Chem. Phys. Lett.* **1993**, *213*, 10. Erratum: Mielke, S. L.; Lynch, G. C.; Truhlar, D. G.; Schwenke, D. W. *Chem. Phys. Lett.* **1994**, *217*, 173.
(38) Stark, K.; Werner, H.-J. *J. Chem. Phys.* **1996**, *104*, 6515.
(39) Hase, W. L.; Duchovic, R. J.; Lu, D.-H.; Swamy, K. N.; Vande Linde, S. R.; Wolf, R. J. *VENUS, A General Chemical Dynamics Computer Program*, 1988.
(40) Bencsura, Á.; Lendvay, G. *Lect. Notes Compu. Sci.* **2004**, *3044*, 290.
(41) Frisch, M. J.; Trucks, G. W.; Schlegel, H. B.; Scuseria, G. E.; Robb, M. A.; Cheeseman, J. R.; Zakrzewski, V. G.; Montgomery, J. A., Jr.; Stratmann, R. E.; Burant, J. C.; Dapprich, S.; Millam, J. M.; Daniels, A. D.; Kudin, K. N.; Strain, M. C.; Farkas, O.; Tomasi, J.; Barone, V.; Cossi, M.; Cammi, R.; Mennucci, B.; Pomelli, C.; Adamo, C.; Clifford, S.; Ochterski, J.; Petersson, G. A.; Ayala, P. Y.; Cui, Q.; Morokuma, K.; Rega, N.; Salvador, P.; Dannenberg, J. J.; Malick, D. K.; Rabuck, A. D.; Raghavachari, K.; Foresman, J. B.; Cioslowski, J.; Ortiz, J. V.; Baboul, A. G.; Stefanov, B. B.; Liu, G.; Liashenko, A.; Piskorz, P.; Komaromi, I.; Gomperts, R.; Martin, R. L.; Fox, D. J.; Keith, T.; Al-Laham, M. A.; Peng, C. Y.; Nanayakkara, A.; Challacombe, M.; Gill, P. M. W.; Johnson, B.; Chen, W.; Wong, M. W.; Andres, J. L.; Gonzalez, C.; Head-Gordon, M.; Replogle, E. S.; Pople, J. A. *Gaussian 98*, revision A.11.4, Gaussian, Inc.: Pittsburgh, PA, 2002.
(42) Hayes, M.; Gustafsson, M.; Mebel, A. M.; Skodje, R. T. *Chem. Phys.* **2005**, *308*, 259.